

Zinc Thiolate Complexes $[\text{ZnL}_n(\text{SR})]^+$ with Azamacrocyclic Ligands, Part III: The Influence of the Ligand L_n on the Reactivity of Zinc-Bound Thiolate^[‡]

Johannes Notni,^[a] Wolfgang Günther,^[a] and Ernst Anders*^[a]

Keywords: Zinc / Sulfur ligands / Kinetics / Density functional calculations / Enzyme models

In this study, we focus on the structure–reactivity relationship of cationic zinc thiolate complexes with the general formula $[\text{Zn}(\text{L}_n)(\text{SR})]\text{ClO}_4$ (L_n : n -dentate azamacrocyclic ligand; R = phenylmethyl). The complexes feature macrocyclic ligands with ring sizes varying from 11 to 16 atoms and possess three or four nitrogen donors (three of them containing one tertiary nitrogen). Thiol methylations with methyl iodide have been performed in order to determine the relative reactivities, because this reaction has been used before to investigate zinc thiolate reactivity and therefore allows comparison of our results with literature data. The kinetic behaviour was investigated in nitromethane and dichloromethane and was found to be second order in all cases. The observed rate constants vary in the range of $k_2 = 2.46\text{--}55.28 \times 10^{-3} \text{ M}^{-1} \text{ s}^{-1}$ in nitromethane and $k_2 = 0.23\text{--}7.35 \times 10^{-3} \text{ M}^{-1} \text{ s}^{-1}$ in dichloromethane at 300 K. Furthermore, the structures of all thiolate complexes were optimised at the B3LYP/6-311+G(d) level of theory. Natural bond orbital (NBO) analyses were performed to obtain information on partial charges of the heteroatoms

and energies of a lone pair in a p-type orbital at the zinc-bound sulfur. In order to elucidate which parameters determine reactivity, selected structural and electronic parameters were correlated with the experimental rate constants. As a result, we found that the reaction is controlled predominantly by frontier orbital energy in dichloromethane and by charge in nitromethane. However, we observed that electronic reactivity control can be overridden by the degree of steric obstruction of the zinc ion, which directly depends on ring size and configuration of the ring nitrogens. The complex $[\text{Zn}(\text{cyclen})(\text{SR})]\text{ClO}_4$ (**5**) can therefore not be included in any of the correlations; steric constraint imposed by the comparably small ring system causes an extraordinarily increased reactivity. In turn, this finding provides a new rationale for the high reactivity reported for the cyclen complex $[\text{Zn}(\text{cyclen})(\text{OH})]^+$, which has been used as a model for carbonic anhydrase in previous studies.

(© Wiley-VCH Verlag GmbH & Co. KGaA, 69451 Weinheim, Germany, 2007)

Introduction

Methylation is of outstanding importance for biosystems.^[2] Irregularities in this process are implicated in the development of the most severe diseases such as cancer, cardiac diseases and neural tube defects. Currently, about 150 methyl transferases (EC 2.1.1.*n*) are known, of which approximately 140 use *S*-adenosylmethionine (SAM) as a methyl donor.^[3] As the SAM precursor methionine is produced (regenerated) by methylation of the thiol function of homocysteine, thiol-methylating enzymes such as the cobalamin-dependent/independent methionine synthases^[4,5] play a crucial role for biological methylation in general. Both require zinc(II) as a cofactor. Other thiol-alkylating enzymes that also feature a zinc centre in their catalytic domain are the Ada DNA repair protein,^[6] farnesyl transfer-

ase,^[7] methanol-CoM-methyltransferase^[8] and betaine-homocysteine *S*-methyltransferase.^[9]

The biological importance of the reactions catalysed by these enzymes led to the development of a variety of zinc(II) complexes as functional model compounds in order to gain better understanding of the reaction mechanism. They all feature at least one zinc-thiolate linkage and one or more additional ligands that are responsible for the overall charge of the complex and the reactivity of the thiolate ligand. For a long time, the mechanism of methylation has been subject to debate. Two substantially different reaction modes have been proposed: an attack of free thiolate after prior dissociation of the complex, and an associative mechanism that includes a four-centre transition structure. The first path would show a first-order kinetic behaviour and the latter is expected to be second-order. However, the observed kinetic behaviour cannot finally prove a proposed mechanism because of possible perturbation effects, which could influence the observed reaction order. In the following, a brief survey of selected important studies on this subject is given.

Wilker and Lippard employed the dianionic tetrathiolate $[\text{Zn}(\text{SPh})_4]^{2-}$ as a functional model for Ada.^[10] They found that methylation of the complex by $(\text{MeO})_3\text{PO}$ yielded

[‡] For further reference see: Zinc Thiolate Complexes $[\text{ZnL}_n(\text{SR})]^+$ with Azamacrocyclic Ligands, Part I: Synthesis and Structural Properties^[1]

[a] Friedrich-Schiller-Universität Jena, Institut für Organische Chemie und Makromolekulare Chemie, Humboldtstr. 10, 07743 Jena, Germany
E-mail: ernst.anders@uni-jena.de

Supporting information for this article is available on the WWW under <http://www.eurjic.org> or from the author.

PhSMe and postulated a dissociative reaction mechanism. This seems particularly plausible as the reaction was carried out in a polar solvent, thus facilitating the dissociation of the thiolate from the highly charged complex anion. Vahrenkamp et al. studied the methylation of tris(pyrazolyl)-boratozinc(II) thiolates $\text{Tp}^{\text{R,R}}\text{ZnSR}$ in chloroform. Investigation of the kinetics provided strong evidence that these reactions occur intramolecularly, featuring a four-centre transition structure.^[11–13] A similar conclusion has been drawn by Carrano et al., who investigated the methylation of a series of scorpionate zinc thiolates.^[14–16] Darenbourg et al. studied alkylations of a zinc complex with a bis-thiolate $[\text{N}_2\text{S}_2]^{2-}$ chelate ligand.^[17] They also obtained the thioether derivatives, but did not discuss the mechanism. Riordan and co-workers investigated the reactivity of zinc thiolates with a borato ligand,^[18] focusing in particular on the influence of additional hydrogen bonds to the thiolate.^[19] They found that hydrogen bonding considerably lowers the nucleophilicity of the thiolates. Similar to the results by Vahrenkamp et al., an associative mechanism is proposed because of the observed second-order kinetic behaviour of the reactions. However, in a recent contribution by Vahrenkamp and co-workers, which covers a comparison of methylation rates of zinc thiolates with N_3 , N_2S , NS_2 and S_3 tripod ligands, evidence is given that a “sulfur-rich” coordination environment is likely to promote a dissociative mechanism.^[20]

In all preceding studies of complexes $[\text{ZnL}_n\text{SR}]$, much attention is paid to the influence of the reactive thiolate ligand on alkylation mechanism and reactivity, or their dependence on different N/S ligations of the zinc ion. In contrast, we focus exclusively on *N*-ligated zinc thiolates. Our interest lies mainly in the coordination geometry and electronic properties of the complexes as reactivity-determining factors. Thus, we address the following questions: What is the actual contribution of L_n to the nucleophilicity of a given thiolate ligand? Is it possible to derive a quantitative relation between structure and reactivity? Which, if any, structural and/or electronic parameters are suitable for the prediction of reactivity?

Recently, we introduced a series of novel zinc thiolate complexes^[1] that are ideally suited for these investigations for several reasons: 11 different compounds meeting the experimental requirements are currently available; they fea-

ture both N_3S and N_4S coordination environments for zinc(II); all compounds are fully characterised by X-ray crystallography; they are insensitive to the influence of air and moisture; reactions with electrophiles (e.g., methyl iodide, benzyl bromide, acetyl and benzoyl chloride, and carbon disulfide^[21]) were found to occur cleanly and on a convenient time scale; they comprise a sufficiently small number of non-hydrogen atoms to be suited for investigation by high-level density functional calculations. The latter instance offers the possibility to reveal the effect especially of electronic parameters that are only accessible by computation, for example, orbital energies and partial charges. This discloses a lot of new perspectives for the interpretation of the reactivity of such complexes.

Results and Discussion

Starting Materials

The alkylation experiments were performed using a series of 11 zinc(II) thiolate complexes with azamacrocyclic ligands of the general formula $[\text{ZnL}_n(\text{S}-\text{CH}_2-\text{C}_6\text{H}_5)]\text{ClO}_4$ (see Figure 1, Table 1). Their syntheses and structures have been reported in detail before.^[1] They contain 11–16-membered azamacrocycles with three (**1–4**) and four (**5–11**) secondary nitrogen donors. In three of them, namely compounds **2**, **4** and **9**, one tertiary nitrogen is incorporated.

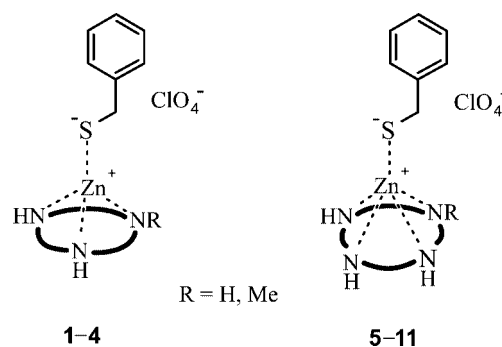


Figure 1. Generic structures of compounds **1–11**. Bold lines indicate alkyl bridges.

Table 1. Macrocyclic ligands of complexes **1–11**, with the general formula $[\text{ZnL}_n(\text{S}-\text{CH}_2-\text{C}_6\text{H}_5)]\text{ClO}_4$.

Compound	L_n abbreviated names	L_n IUPAC names
1	[11]aneN ₃	1,4,8-triazacycloundecane
2	methyl-[11]aneN ₃	8-methyl-1,4,8-triazacycloundecane
3	[12]aneN ₃	1,5,9-triazacyclododecane
4	methyl-[12]aneN ₃	1-methyl-1,5,9-triazacyclododecane
5	[12]aneN ₄ (cyclen)	1,4,7,10-tetraazacyclododecane
6	[13]aneN ₄	1,4,7,11-tetraazacyclotridecane
7	[14]aneN ₄ (cyclam)	1,4,8,11-tetraazacyclotetradecane
8	<i>i</i> [14]aneN ₄ (<i>iso</i> -cyclam)	1,4,7,11-tetraazacyclotetradecane
9	methyl- <i>i</i> [14]aneN ₄	11-methyl-1,4,7,11-tetraazacyclotetradecane
10	[15]aneN ₄	1,4,8,12-tetraazacyclopentadecane
11	[16]aneN ₄	1,5,9,13-tetraazacyclohexadecane

Methylation Kinetics

For the determination of the reactivities we used the standard model reaction, methylation with methyl iodide, which yielded the corresponding iodide complexes and phenyl methyl sulfide [Equation (1)].



At 300 K, the reactions come to completion within times of hours up to several days. No evidence for the formation of any byproducts was detected. Reaction monitoring could thus easily be performed using NMR spectroscopy. However, this required sufficiently concentrated solutions (0.02 M). In this respect, the varying solubilities of the model complexes proved to be a problem, as rate constants are only suited for direct comparison in case reactions are carried out in the same solvent. We initially intended to investigate the methylation in a nonpolar solvent in order to rule out a dissociative reaction mechanism. This was found to be unfeasible as only five compounds were soluble in chloroform and seven in dichloromethane. However, the semipolar solvent nitromethane could be used for all complexes. Second-order kinetic behaviour was observed in each case (with correlation coefficients of $R^2 > 0.99$ for all fit curves), thus indicating only associated reactions as proposed previously. In this work, we focus on kinetic data obtained from reactions in $[\text{D}_3]\text{nitromethane}$ and $[\text{D}_2]\text{-dichloromethane}$ solution.

Table 2 shows the experimentally determined second-order rate constants of methylation according to Equation 1. As expected, in the more polar solvent nitromethane the reactions proceed several times faster. The factor of acceleration by the solvent varies by about 3 for compound **11** and about 21 for **4**. We currently cannot give an explanation for this remarkable difference. However, the observed rate constants exhibit an even more pronounced dependence on the nature of the azamacrocycle. The fastest reaction in nitromethane was observed for complex **5**, which reacted more than 22 times faster than its slowest competitor, compound **2**. This effect is even more pronounced in dichloromethane; complex **11** reacts faster than **4** by a factor of 32. Because compound **5** is insoluble in this solvent, these data are of limited significance. Hence, a straightforward comparison of the two data sets is not possible in this way.

Table 2. Second-order rate constants of the methylation of compounds **1–11** at 300 K. Values are given in $10^{-3} \text{ M}^{-1} \text{ s}^{-1}$.

Compound	In CD_3NO_2	In CD_2Cl_2
1	4.71	–
2	2.46	0.28
3	7.05	–
4	4.92	0.23
5	55.28	–
6	29.03	–
7	21.60	1.52
8	13.93	1.00
9	8.66	0.53
10	16.69	2.81
11	23.12	7.35

A more expressive representation is given in Figure 2. It shows a comparison of the rate constants of all complexes that could be measured in both solvents. Again it is obvious that the absolute acceleration factor by a more polar solvent is not constant. Rather, a trend is reproduced, and compound **7** is the single exception. An explanation could be the following: The macrocycle cyclam ($[\text{14}]_{\text{ane}}\text{N}_4$), which is featured in complex **7**, forms particularly stable tetra-coordinate zinc complexes. The ring size of 14 atoms and the configuration of the *N*-bound hydrogen atoms in the complex enable the placement of the zinc ion in the plane of the four nitrogens^[22] (a structural representation of **7** is given in the literature^[1]). In the case of other ligands, a displacement is rather unavoidable. This renders the Zn–S bond of **7** less stable than in the other compounds regarded in this study. A similar conclusion can also be drawn from the mass spectra of the complexes.^[1] In a polar solvent such as nitromethane, the Zn–S bond of **7** is weakened above average (without an actual dissociation taking place) and the reaction receives particular acceleration. Thus we conclude that the observed order of reaction rates obviously arises from a superposition of ligand and solvent control, but the macrocyclic ligand has the predominant influence on the reactivity of the thiolate. In addition, we found that the complexes with a tertiary nitrogen (**2**, **4** and **9**) exhibit a slightly reduced rate constant (by about 30–50%) compared to the analogue compounds without the methyl groups (**1**, **3** and **8**, respectively; see Table 2). The effect can be observed for both solvents.

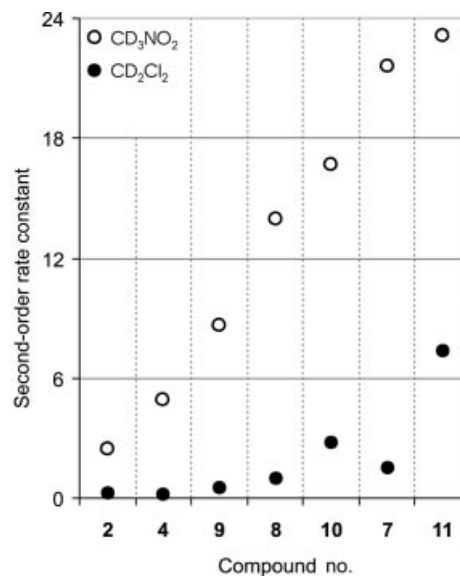


Figure 2. Comparison of second-order rate constants (given in $10^{-3} \text{ M}^{-1} \text{ s}^{-1}$) of the reactions with methyl iodide in CD_2Cl_2 and CD_3NO_2 . Only the data of compounds that are soluble in both solvents are plotted.

Density Functional Calculations

Different methods can be applied to obtain structural information, such as spectroscopy, computation or X-ray crystallography. However, the structural information pro-

vided by the latter is only of restricted use for the interpretation of processes in solution. In most cases, spectroscopic methods can be applied to solutions as well, but the structural information it provides is restricted to certain parameters and of limited generality. The search for parameters suitable to correlate to the experimentally determined reaction rates requires detailed information on the nature of the zinc–sulfur bond and the electronic properties of the sulfur atom that is not accessible by either spectroscopy or crystallography. Thus, quantum mechanical calculation is the method of choice to obtain structural and electronic data for correlation purposes. A comparable approach has been successfully applied by Halfen, Brunold et al., who investigated the electronic structure of 4-methylphenylthiolate and some transition-metal complexes thereof by density functional calculations in order to obtain an explanation for the observed nucleophilicities.^[23]

An investigation that provided an accurate description of the observed reactivities would require more than gas-phase optimisations of the starting material complexes. Rather, a calculation of the transition state of the nucleophilic attack, including the modelling of solvent effects, had to be performed for the methylation reaction of every single compound. However, such calculations would by far push the boundary of the currently available computational resources. In addition, all our previous attempts to locate the transition states failed because of the extremely flat potential energy hypersurface. Thus, only gas-phase structures could be calculated at a sufficient level of theory, that is, one that includes polarised and diffuse functions, which are necessary for the correct description of coordination compounds. We were thus searching for a simple but effective means of characterising the observed reactivities using only the available structural and electronic data derived from gas-phase calculations. At least, we do not expect problems concerning the geometries obtained. According to our own experience, in the case of azamacrocyclic-zinc(II) complexes, there are generally only minute differences between the structures obtained by calculations in the gas phase and in the presence of solvents.

We decided to use density functional theory because it is also applicable to larger molecules. All structures were optimised in the gas phase at the B3LYP/6-311+G(d) level of theory, with the molecular structures derived from X-ray diffraction^[1] as starting geometries. The experimental and computational structures are in reasonable accordance. As expected, minor deviations in bond lengths and differences in the conformations (e.g., rotations about the Zn–S bond) were observed. Natural bond orbital (NBO)^[24] analyses were performed for all structures to obtain information on orbital energies and partial charges on the metal and the heteroatoms. The energy of a specific lone pair orbital at the sulfur atom was determined, the reason for this being the following: In a previous study, it has been shown that a zinc-bound oxygen atom in complexes $[\text{LZn}-\text{OH}]^+$ possesses three lone pairs: two of sp hybridisation and one of pure p character.^[25] The latter one is the orbital with the highest energy, and because of its orientation, it is re-

sponsible for nucleophilic attack. A higher energy implicates a smaller energy gap between this orbital and the LUMO of an electrophilic substrate, thus facilitating orbital interaction and lowering transition-state energy. A comparable configuration was found for the zinc thiolate complexes. There are three localised orbitals at the zinc-bound sulfur atom, two with sp and one with a pure (>99%) p character, which also possesses the highest energy. Its strictly localised character has been proven for all structures regarded in this study. No significant overlap with other orbitals that would indicate multicentre bonding could be detected. It is thus reasonable to assume that the energy of this “localised HOMO” could be a controlling factor for the nucleophilic reactivity.

Correlations

In the following consideration, we focus on possible correlations of computed parameters with the experimentally determined rate constants. We thus refer to three parameters based on gas-phase calculations that are likely to correlate with thiolate reactivity: the Zn–S bond length, the S atom partial charge and the above-mentioned S lone pair orbital energy.

As the Zn–S bond length reflects how tightly the thiolate is bound and how much its reactivity is lowered by zinc(II) complexation, one would expect it to be a good measure for reactivity. Figure 3 depicts the result, the rate constants of methylation plotted against the computed Zn–S bond lengths. There is apparently only a very loose correlation, which is certainly not sufficient for a quantitative description of reactivity. (Two points that correspond to compounds **5** and **6** are highlighted by means of square shaping in this and other charts; this is of importance and will be explained below.)

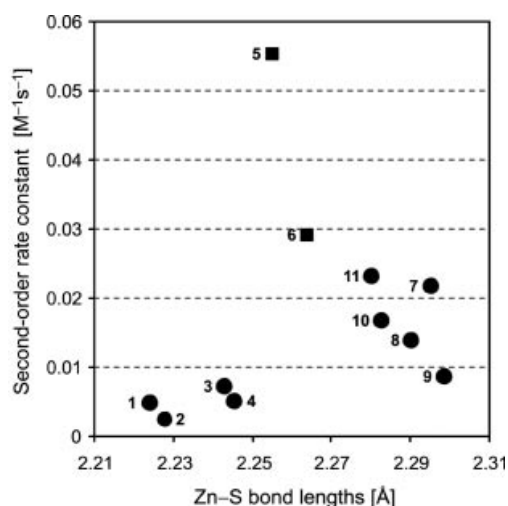


Figure 3. Second-order rate constants of thiolate methylation, plotted against the Zn–S bond lengths; solvent: nitromethane.

A much more promising situation is found for the plots of the sulfur's partial charge (see Figure 4). The data points for the reaction in nitromethane (with exception of **5** and

6) are found on a steady curve. In principle, this allows a prediction of reactivity: A larger absolute value of partial charge implicates an increased nucleophilic reactivity. The line that indicates this dependency is a spline curve, simply chosen by an obviously visible regularity of the data points. Of course, its existence does not permit any conclusions beyond the fact that there is a systematic relation between the two parameters regarded. It is also obvious that in the less polar solvent dichloromethane, such a correlation does not exist.

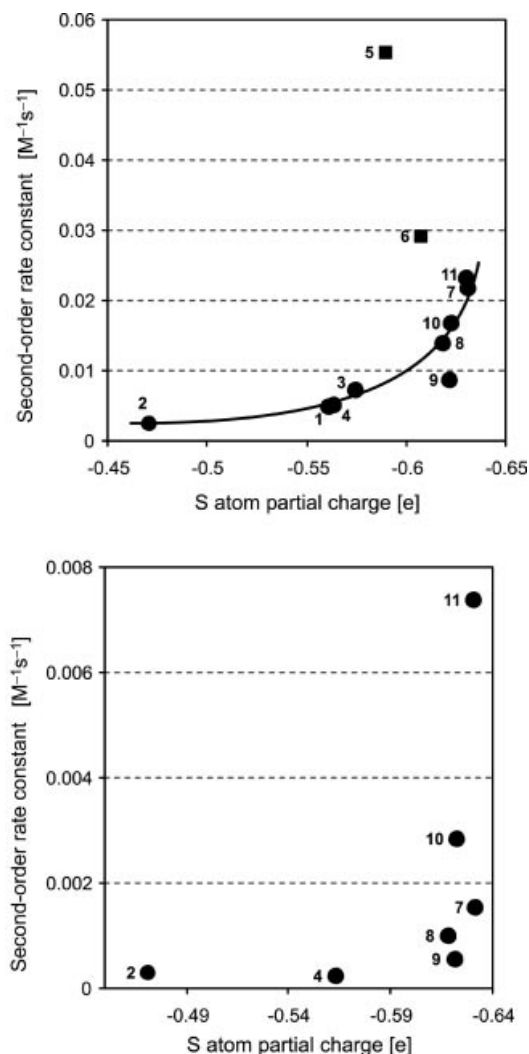


Figure 4. Second-order rate constants of thiolate methylation, plotted against partial charges of the sulfur atom. Upper diagram: solvent nitromethane; lower diagram: solvent dichloromethane.

The energy of the *p*-type lone pair seems to be a good measure for thiolate reactivity in both solvents (although again two exceptions, 5 and 6, are encountered). As can be seen in Figure 5, the regularity is more pronounced in dichloromethane. The LP energy is the only parameter that allows a correlation with the rate constants for this solvent at all.

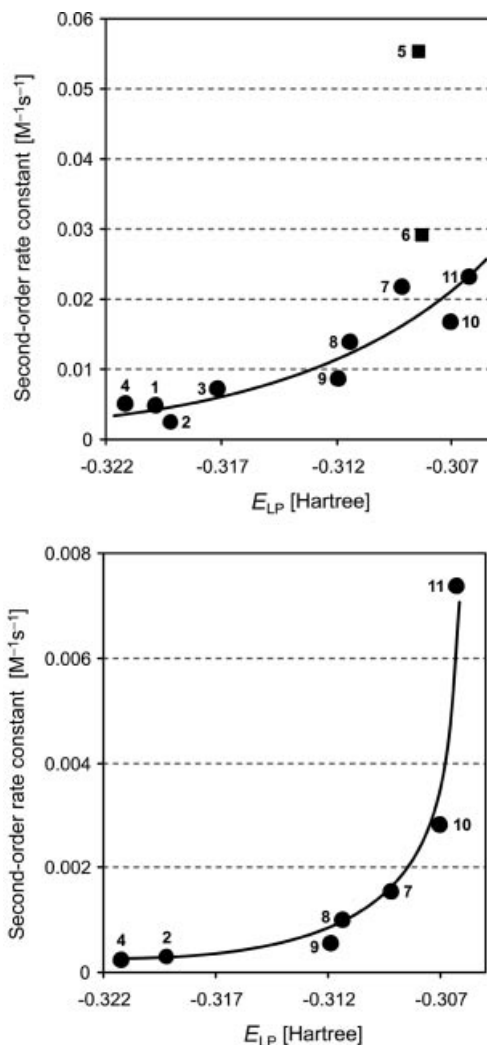


Figure 5. Second-order rate constants of thiolate methylation, plotted against energies of the sulfur's *p*-type lone pair. Upper diagram: solvent nitromethane; lower diagram: solvent dichloromethane.

All these findings allow some interesting conclusions: (1) Justifying solely from structural parameters (bond lengths), it is not possible to draw conclusions regarding the reactivity; one has to employ other sources of data, such as quantum mechanical calculation. (2) Obviously, the reaction can be biased towards charge or orbital control, depending on the polarity of the solvent. In nitromethane, both parameters (partial charge and orbital energy) are useful to describe the reactivity; in dichloromethane, the reaction is predominantly orbital-controlled. (3) The observed regularities include both N_3S and N_4S systems. The concept is obviously not restricted to a specific coordination environment of zinc(II) but is apparently valid for zinc thiolates in general.

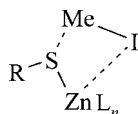
However, we would like to emphasise that the correlations discussed herein are not supported by any equations or a stringent theory. This would of course not be permissible, as the results of gas-phase calculations are used in combination with data obtained from experiments in solu-

tion. Notwithstanding this background, some fundamental conclusions can be drawn, as will be demonstrated in the following.

Steric Influences

Until now, we have not discussed the rate constants obtained for compounds **5** and **6**, which are indicated by squares in Figure 3, Figure 4 and Figure 5 (a structural representation of their calculated geometries is given in Figure 7, see below). Their reactivities differ significantly from those of the other complexes. They exhibit the largest rate constants whilst showing only average values for the structural and electronic parameters. Thus, we conclude that reactivity is also controlled by another important factor.

Regarding the reaction mechanism, we share the predominant viewpoint from the literature, the assumption that the methylation reaction involves an attack of the zinc-bound thiolate and features a four-centre intermediate (Scheme 1).^[12–15,26,27] In this case, the methylation (as well as any other reaction) is restricted to occur at the thiolate side of the complex cation. As the coordination of the reacting molecules to Zn^{II} implicates a steric demand, the degree of obstruction of the zinc(II) ion by the macrocycle should have a pivotal influence on the geometry of the transition state.



Scheme 1. Assumed four-centred transition state of the methylation of zinc-bound thiolate.

In case of planar chelate ligands, the degree of surface obstruction of a metal ion caused by complexation can easily be characterised by the bite angle; in case the ligand's donor atoms and the metal ion form a four-sided pyramid, one rather has to consider the solid angle at the Zn vertex. It is usually given in steradian [*sr*] and represents a measure for the extent to which the zinc ion is displaced out of the plane (or near-plane) of the four N atoms. In theory, values can vary between 0 *sr* (for infinite Zn–N distance) and 2π *sr* (for in-plane location of Zn^{2+}).^[28] The results of these considerations are summarised in Figure 6, which also shows calotte model representations in order to illustrate the varying degree of steric demand of the macrocyclic ligands.

With regard to the comparably small solid angle of 0.95 π *sr* associated to compound **5**, it is obvious that its coordination geometry can be assessed as being quite distorted in comparison to the other N_4Zn systems (Figure 7). The calotte model drawings also show that the zinc ion in **5** is a lot more exposed. However, in the case of compound **6**, the solid angle is comparable to other N_4 complexes. As the corresponding calotte drawing still indicates a substantial degree of exposition of the metal ion, there is apparently another structural factor that affects the steric situation: the

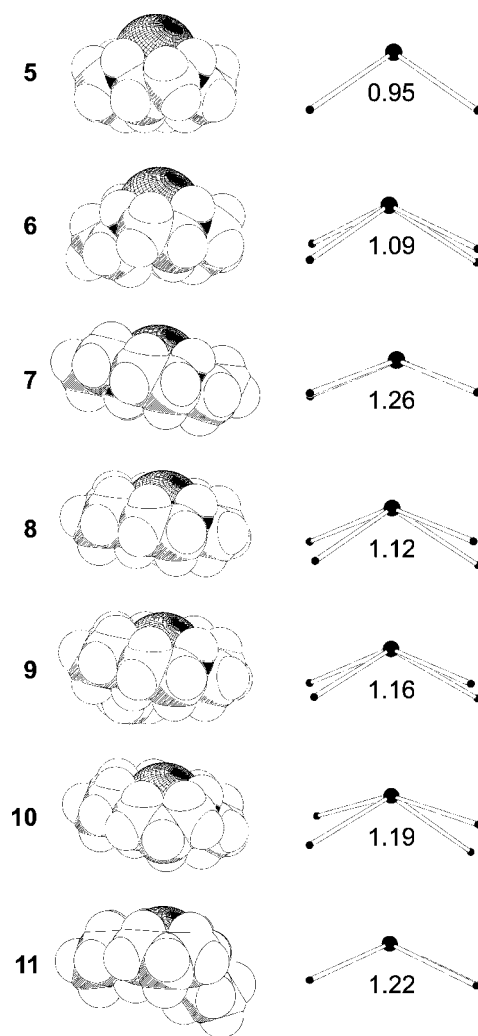


Figure 6. Left column: calotte model drawings of the cations of compounds **5**–**11**, thiolate ligands omitted. Right column: N_4Zn coordination polyhedra and solid angles at the Zn vertex [π *sr*] of the same molecules; the perspective of vision corresponds to the drawings in the left column. All representations are derived from the calculated structures (see computational details).

configuration of the nitrogen atoms of the macrocycle. (In a previously published study, we discussed this aspect in detail, and structural representations of complexes **1**–**11** are given therein.^[1]) Of the N_4 systems **5**–**11**, compounds **5** and **6** are the only examples in which all N-bound hydrogen atoms are located at the thiolate side [the (+)-side] of the molecule [the so-called (+ + + +)-configuration, see also Figure 7]. This characteristic accessorily accounts for a smaller degree of steric hindrance, as a hydrogen atom on the (+)-side obstructs the zinc(II) ion to a lesser extent than an alkyl bridge.

As a result of a superposition of both the ring size and configuration effects, complex **5** exhibits a markedly superior reactivity, while the just slightly increased reactivity of compound **6** is mainly based on the all-(+) configuration of the macrocycle. Moreover, a plausible mechanistic interpretation can be given for this acceleration: Given a more exposed zinc(II) ion, formation of a four-centred transition

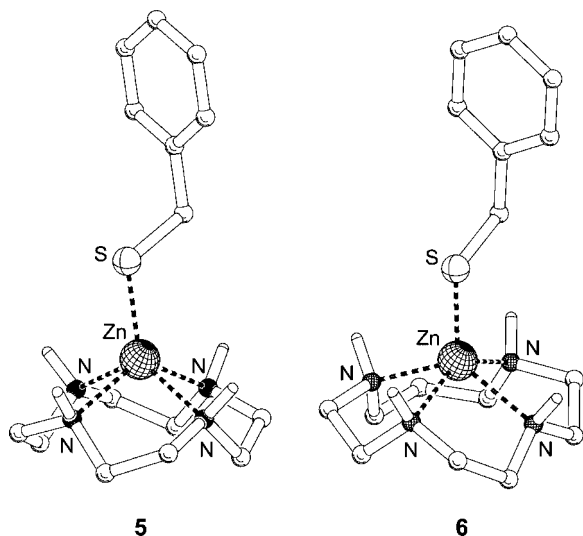


Figure 7. Structures of compounds **5** and **6**, calculated at the B3LYP/6-311+G(d) level of theory. Hydrogen atoms on carbon atoms are omitted for clarity of presentation. Note the good correlation of the values of the critical Zn–S bond lengths obtained by experimental and DFT calculation [for **5**: exp. 2.266(2) Å, calcd. 2.25 Å; for **6**: exp. 2.2853(9) Å, calcd. 2.26 Å].

state is facilitated rather than in the case of highly obstructed zinc(II), as illustrated in Figure 8. The latter would promote the formation of a more linear transition state that entails separation of the resulting iodide anion from the cationic centre, thus leading to a higher energy barrier for the overall reaction. Nevertheless, we do not expect this difference to amount to more than a couple of kilocalories per mole. However, as a small decrease of transition-state energy of 1.5 kcal mol^{−1} already results in an increase of reaction velocity of about one order of magnitude, this allows for a sound explanation of the observed differences in reaction velocity.

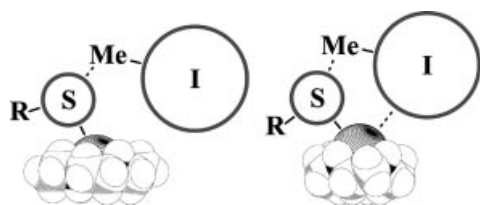


Figure 8. Illustration of possible differences in transition-state geometries for the nucleophilic attack of zinc-bound thiolate on methyl iodide. As examples, calotte model drawings of the ZnL_n moieties of **7** (left) and **5** (right) were utilised. Ion radii of S and I are not exactly fitted to the ion radii of the calotte models.

Conclusions

General Remarks

The thiolate complexes have proven to be suitable functional models for thiolate-methylating enzymes. As expected, a clean second-order methylation reaction was found. The observed acceleration of the reaction in a polar environment comes as no surprise; neither do the general

results concerning charge and orbital control in the different solvent systems. Similar observations have been reported by many other work groups (see above). However, an important improvement provided by our work is the presented way of analysing experimental reactivity data by correlation to electronic parameters obtained from gas-phase density functional calculations. It enabled us to elucidate to what extent certain geometry factors can influence reactivity and override electronic and/or orbital control. With regard to the rapidly increasing availability of computing power, this technique could generally prove to be a valuable tool in exploring structure–reactivity relationships and catalyst tailoring. However, we are aware that our procedure is only a coarse approximation. As mentioned above, an exact treatment of the subject would require DFT calculations of the transition states of the methyl iodide reactions for all investigated complexes, a task that we found to be unfeasible. We believe, however, that even though our approach is quite coarse, it provides interesting insight into the chemistry of nucleophilic cationic complexes.

Implications Concerning CA Model Compounds

The unexpected reactivities of compounds **5** and **6** (Figure 7) allow some additional conclusions of high interest. Although it may not seem that this work relates to the enzyme carbonic anhydrase (CA), it nevertheless provides fundamentally enhanced insight into the chemistry of CA model compounds.

Carbonic anhydrases (CA) are a family of zinc enzymes that accelerate the reversible hydration of CO₂ by a factor of up to 10⁷ as compared to the uncatalysed reaction.^[29,30] The catalytic domain consists of a zinc(II) ion that is bound to three histidine residues and bears an additional water molecule or hydroxide ligand (dependent from pH). The properties of this structural motif have been elucidated using a variety of monodentate zinc hydroxide complexes.^[31–35] In addition, numerous experimental^[36–38] and computational studies provided detailed insight into the reaction mechanism.^[39–42]

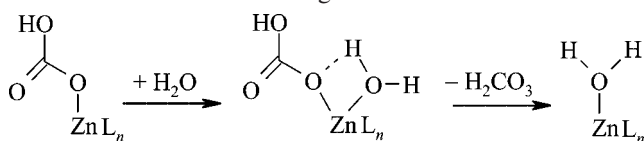
In 1995, van Eldik and co-workers^[43] published a study addressing the reaction rates of several functional CA model complexes of the general formula [ZnL_n(OH)]⁺ with CO₂, according to Equation (2).



They investigated complexes of various chelate ligands L_n, of which two macrocycles with four nitrogen donors are of particular interest. One is 14-membered (comparable to the ligand in compound **8**), and the other is cyclen as in compound **5**. They found that the CO₂ hydration velocity of the latter exceeds that observed for the first by a factor of approximately 15. However, no explanation for this remarkable variation is given. With regard to the results of the present work, we would like to propose a rationale for these observations, as, because of the close structural relationship of the ligands, we assume the steric situation for

those hydroxo complexes is comparable to compounds **8** and **5**, respectively.

In a previous study, some of us have shown that the aquation of zinc hydrogencarbonato complexes involves an intramolecular proton transfer as depicted in Scheme 2.^[42] It involves the initial coordination of a water ligand to the zinc centre, which then protonates the hydrogen carbonate. Subsequently, carbonic acid is expelled (which, under normal conditions, will immediately be deprotonated in the reaction medium) and the hydroxo complex $[\text{ZnL}_n(\text{OH})]^+$ is obtained. In the course of this mechanism, only uncharged molecules dissociate from the metal centre. However, with an increasing steric demand of the chelate ligand, the aquation may as well afford a preliminary dissociation of hydrogen carbonate, followed by addition of water, which is subsequently deprotonated. This dissociative reaction pathway necessarily includes a separation of electrical charges, which is very likely to result in an increased reaction barrier. In practice, one will normally encounter hybrid forms of both idealised mechanism types that are more or less biased to one side. We thus assume, by analogy with the results of the present work, that in the case of aquation of the two hydrogencarbonato complexes, the exposed placement of the zinc ion in the cyclen complex is much more likely to promote the associated reaction mechanism, thereby lowering the reaction barrier and increasing the aquation rate. We therefore conclude that the unique combination of properties united by the zinc(II) complexes of the ligand cyclen, that is, a small solid angle of the coordination polyhedron and the all-(+) configuration of the *N*-bound hydrogen atoms, results in an extraordinarily increased reactivity of additional monodentate ligands.



Scheme 2. Calculated mechanism of the aquation of zinc(II) hydrogencarbonato complexes.^[41]

Experimental Section

General: The thiolate complexes were prepared according to our published procedure.^[1] Deuterated solvents were obtained from eurisotop. NMR spectra were recorded with a BRUKER AC 400 spectrometer at a temperature of 300 K.

Methylation Kinetics: The complex (0.1 mmol) was dissolved in deuterated solvent (5 mL) (CD_2Cl_2 or CD_3NO_2). Methyl iodide (0.1 mmol) was added with a microlitre syringe. After short stirring, a sample of the solution was placed in a sealable NMR tube and inserted into the spectrometer. ^1H NMR spectra were recorded every 30 min for dichloromethane and every 15 min for nitromethane solutions. For determination of the rate constants of nitromethane solutions of **6**, **7** and **10**, the decreasing integral of the methyl peak of methyl iodide was utilised. For all other measurements, the signals assigned to benzylic protons of the zinc-bound thiolate were used for integration. In all cases, the integral of all aromatic peaks was taken as a reference, as it was assumed to be

constant. Thus, concentration data for kinetic analysis could be obtained directly from the standardised integral values. Under the condition that the reaction proceeds according to Equation (1) and the reactants are present in equal concentrations, a special case of a second-order kinetic law can be applied [Equation (3)].

$$1/c - 1/c_0 = k_2 t \quad (3)$$

In this equation, c_0 represents the initial concentration of any reactant and c is the concentration of any reactant at a given time t . Accordingly, the obtained concentration data were plotted against t and a linear function was obtained by regression analysis. Linear correlations were found in all cases, exhibiting correlation coefficients of $R > 0.995$. The second-order rate constants were obtained from the slopes of these fit functions.

Computational Details: Full geometry optimisations, that is, without constraints, were carried out using the Gaussian98^[44] program package (Rev. A11/4). All optimisations were performed using the hybrid B3LYP^[45] density functional method, which includes the use of a term that accounts for the effect of dynamic electron correlation (Coulomb hole).^[46] Geometries were optimised in the gas phase using the standard 6-311+G(d) basis set. All structures were rigorously characterised as true minima. NBO analyses^[24,47] were carried out using version 5.0 of the NBO program^[48] as patched in Gaussian98. A search for three-centre, four-electron hyperbonds using the keyword 3CHB yielded no evidence of nonlocalised orbitals. The partial charges of the heteroatoms were obtained by natural population analysis. Orbital energies were taken from the Natural Bond Orbital Summary Table.

Supporting Information (see also the footnote on the first page of this article): Mathematical details on calculation of the solid angle, a table with absolute energies (SCF energies, ΔU , ΔG) and cartesian coordinates in xyz format of all computed structures are given.

Acknowledgments

Financial support of this work by the Deutsche Forschungsgemeinschaft, SFB 436 “Metal Mediated Reactions Modeled after Nature” is gratefully acknowledged. We particularly thank Prof. Dr. M. Westerhausen (FSU Jena) for an enlightening discussion, Dr. Stephan Schenk (ETH Zürich) for his advice concerning computational problems, and Steffen Kluge (FSU Jena) for his assistance in mathematics.

- [1] J. Notni, H. Görls, E. Anders, *Eur. J. Inorg. Chem.* **2006**, 1444–1455.
- [2] Z. S. Zhou, G. Zhao, W. Wan in *Frontiers of Biotechnology and Pharmaceuticals* (Eds.: H. Guo, R. Zhao), China Scientific Book Services, Beijing, China, **2001**, vol. 2, chapter 3, pp. 199–217.
- [3] *Expasy Proteomics Server*, <http://www.expasy.org>.
- [4] V. L. Schramm, *Curr. Opin. Chem. Biol.* **1997**, 1, 323–331.
- [5] K. Peariso, Z. S. Zhou, A. E. Smith, R. G. Matthews, J. E. Penner-Hahn, *Biochemistry* **2001**, 40, 987–993.
- [6] L. C. Myers, M. P. Terranova, A. E. Ferentz, G. Wagner, G. L. Verdine, *Science* **1993**, 261, 1164–1167.
- [7] H.-W. Park, S. R. Boduluri, J. F. Moomaw, P. J. Casey, L. S. Beese, *Science* **1997**, 275, 1800–1805.
- [8] K. Sauer, R. K. Thauer, *Eur. J. Biochem.* **1997**, 249, 280–285.
- [9] A. P. Breksa III, T. A. Garrow, *Biochemistry* **1999**, 38, 13991–13998.
- [10] J. J. Wilker, S. J. Lippard, *Inorg. Chem.* **1997**, 36, 969–978.
- [11] R. Burth, H. Vahrenkamp, *Z. Anorg. Allg. Chem.* **1998**, 624, 381–385.

- [12] U. Brand, M. Rombach, J. Seebacher, H. Vahrenkamp, *Inorg. Chem.* **2001**, *40*, 6151–6157.
- [13] M. Ji, B. Benkmil, H. Vahrenkamp, *Inorg. Chem.* **2005**, *44*, 3518–3523.
- [14] B. S. Hammes, C. J. Carrano, *Inorg. Chem.* **1999**, *38*, 4593–4600.
- [15] B. S. Hammes, C. J. Carrano, *Inorg. Chem.* **2001**, *40*, 919–927.
- [16] J. N. Smith, Z. Shirin, C. J. Carrano, *J. Am. Chem. Soc.* **2003**, *125*, 868–869.
- [17] C. A. Grapperhaus, T. Tuntulani, J. H. Reibenspies, M. Y. Darsensbourg, *Inorg. Chem.* **1998**, *37*, 4052–4058.
- [18] S.-J. Chiou, J. Innocent, C. G. Riordan, K.-C. Lam, L. Liable-Sands, A. L. Rheingold, *Inorg. Chem.* **2000**, *39*, 4347–4353.
- [19] S.-J. Chiou, C. G. Riordan, A. L. Rheingold, *Proc. Natl. Acad. Sci. USA* **2003**, *100*, 3695–3700.
- [20] M. Rombach, J. Seebacher, M. Ji, G. Zhang, G. He, M. M. Ibrahim, B. Benkmil, H. Vahrenkamp, *Inorg. Chem.* **2006**, *45*, 4571–4575.
- [21] J. Notni, S. Schenk, A. Roth, W. Plass, H. Görls, U. Uhlemann, A. Walter, M. Schmitt, J. Popp, S. Chatzipapadopoulos, T. Emmeler, H. Breitzke, J. Leppert, G. Buntkowsky, K. Kempe, E. Anders, *Eur. J. Inorg. Chem.* **2006**, 2783–2791.
- [22] A. W. Addison, E. Sinn, *Inorg. Chem.* **1983**, *22*, 1225–1228.
- [23] D. C. Fox, A. Fiedler, H. L. Halfen, T. C. Brunold, J. A. Halfen, *J. Am. Chem. Soc.* **2004**, *126*, 7627–7638.
- [24] A. E. Reed, R. B. Weinstock, F. Weinhold, *J. Chem. Phys.* **1985**, *83*, 735–746.
- [25] M. Bräuer, J. L. Pérez-Lustres, J. Weston, E. Anders, *Inorg. Chem.* **2002**, *41*, 1454–1463.
- [26] M. Rombach, H. Vahrenkamp, *Inorg. Chem.* **2001**, *40*, 6144–6150.
- [27] H. Brombacher, H. Vahrenkamp, *Inorg. Chem.* **2004**, *43*, 6042–6049.
- [28] For more detailed information on the mathematical background see Supporting Information.
- [29] F. Botre, G. Gros, B. T. Storey (Eds.), *Carbonic Anhydrase*, VCH Publishers, New York, **1991**.
- [30] I. Bertini, C. Luchinat, W. Maret, M. Zeppezauer (Eds.), *Zinc Enzymes*, Birkhäuser, Boston, **1986**.
- [31] G. Parkin, *Chem. Rev.* **2004**, *104*, 699–767.
- [32] E. Kimura, *Acc. Chem. Res.* **2001**, *34*, 171–179.
- [33] X. Zhang, R. van Eldik, T. Koike, E. Kimura, *Inorg. Chem.* **1993**, *32*, 5749–5755.
- [34] A. Looney, G. Parkin, R. Alsfasser, M. Ruf, H. Vahrenkamp, *Angew. Chem. Int. Ed. Engl.* **1992**, *31*, 92–93; *Angew. Chem.* **1992**, *104*, 57–58.
- [35] A. Looney, R. Han, K. McNeill, G. Parkin, *J. Am. Chem. Soc.* **1993**, *115*, 4690–4697.
- [36] D. W. Christianson, C. A. Fierke, *Acc. Chem. Res.* **1996**, *29*, 331–339.
- [37] D. N. Silverman, S. Lindskog, *Acc. Chem. Res.* **1988**, *21*, 30–36.
- [38] J.-Y. Liang, W. N. Lipscomb, *Biochemistry* **1988**, *27*, 8676–8682.
- [39] A. Bottoni, C. Z. Lanza, G. P. Miscione, D. Spinelli, *J. Am. Chem. Soc.* **2004**, *126*, 1542–1550.
- [40] C. S. Tautermann, M. J. Loferer, A. F. Voegelé, K. R. Liedl, *J. Phys. Chem. B* **2003**, *107*, 12013–12020.
- [41] Z. Smedarchina, W. Siebrand, A. Fernández-Ramos, Q. Cui, *J. Am. Chem. Soc.* **2003**, *125*, 243–251.
- [42] M. Mauksch, M. Bräuer, J. Weston, E. Anders, *ChemBioChem* **2001**, *2*, 190–198.
- [43] X. Zhang, R. van Eldik, *Inorg. Chem.* **1995**, *34*, 5606–5614.
- [44] M. J. Frisch, G. W. Trucks, H. B. Schlegel, G. E. Scuseria, M. A. Robb, J. R. Cheeseman, V. G. Zakrzewski, J. A. Montgomery Jr, R. E. Stratmann, J. C. Burant, S. Dapprich, J. M. Millam, A. D. Daniels, K. N. Kudin, M. C. Strain, O. Farkas, J. Tomasi, V. Barone, M. Cossi, R. Cammi, B. Mennucci, C. Pomelli, C. Adamo, S. Clifford, J. Ochterski, G. A. Petersson, P. Y. Ayala, Q. Cui, K. Morokuma, N. Rega, P. Salvador, J. J. Dannenberg, D. K. Malick, A. D. Rabuck, K. Raghavachari, J. B. Foresman, J. Cioslowski, J. V. Ortiz, A. G. Baboul, B. B. Stefanov, G. Liu, A. Liashenko, P. Piskorz, I. Komaromi, R. Gomperts, R. L. Martin, D. J. Fox, T. Keith, M. A. Al-Laham, C. Y. Peng, A. Nanayakkara, M. Challacombe, P. M. W. Gill, B. Johnson, W. Chen, M. W. Wong, J. L. Andres, C. Gonzalez, M. Head-Gordon, E. S. Replogle, J. A. Pople, *Gaussian98*, revision A.11–4, **2002**, Gaussian, Inc., Pittsburgh, PA, <http://www.gaussian.com>.
- [45] A. D. Becke, *J. Chem. Phys.* **1993**, *98*, 5648–5652.
- [46] C. Lee, W. Yang, R. G. Parr, *Phys. Rev. B: Condens. Matter* **1988**, *37*, 785–789.
- [47] A. E. Reed, L. A. Curtiss, F. Weinhold, *Chem. Rev.* **1988**, *88*, 899–926.
- [48] F. Weinhold, *NBO*, version 5, <http://www.chem.wisc.edu/~nbo5/>.

Received: October 13, 2006

Published Online: January 16, 2007